Multifunctional Bi2ZnOB2O6 single crystals for second and third order nonlinear optical applications

Konstantinos Iliopoulos, D. Kasprowicz, Andrzej Majchrowski, E. Michalski, Denis Gindre, Bouchta Sahraoui

AIP | Applied Physics Letters

Multifunctional Bi2ZnOB2O6 single crystals for second and third order nonlinear optical applications

K. Iliopoulos, D. Kasprowicz, A. Majchrowski, E. Michalski, D. Gindre, and B. Sahraoui

Citation: Applied Physics Letters **103**, 231103 (2013); doi: 10.1063/1.4837055
View online: http://dx.doi.org/10.1063/1.4837055
View Table of Contents: http://scitation.aip.org/content/aip/journal/apl/103/23?ver=pdfcov
Published by the AIP Publishing

Multifunctional $Bi_2ZnOB_2O_6$ single crystals for second and third order nonlinear optical applications

K. Iliopoulos,[1,2] D. Kasprowicz,[3] A. Majchrowski,[4] E. Michalski,[5] D. Gindre,[1] and B. Sahraoui[1,a)]

[1]*LUNAM Université, Université d'Angers, CNRS UMR 6200, Laboratoire MOLTECH-Anjou, 2 Bd Lavoisier, 49045 Angers Cedex, France*
[2]*Institute of Chemical Engineering Sciences, Foundation for Research and Technology Hellas (FORTH/ICE-HT), 26504 Patras, Greece*
[3]*Faculty of Technical Physics, Poznan University of Technology, Nieszawska 13 A, 60-965 Poznan, Poland*
[4]*Institute of Applied Physics, Military University of Technology, Kaliskiego 2, 00-908 Warszawa, Poland*
[5]*Institute of Optoelectronics, Military University of Technology, Kaliskiego 2, 00-908 Warszawa, Poland*

(Received 17 October 2013; accepted 15 November 2013; published online 3 December 2013)

$Bi_2ZnOB_2O_6$ nonlinear optical single crystals were grown by means of the Kyropoulos method from stoichiometric melt. The second and third harmonic generation (SHG/THG) of $Bi_2ZnOB_2O_6$ crystals were investigated by the SHG/THG Maker fringes technique. Moreover, SHG microscopy studies were carried out providing two-dimensional SHG images as a function of the incident laser polarization. The high nonlinear optical efficiency combined with the possibility to grow high quality crystals make $Bi_2ZnOB_2O_6$ an excellent candidate for photonic applications. © *2013 AIP Publishing LLC*. [http://dx.doi.org/10.1063/1.4837055]

Recently, there is a growing interest for materials with important second and third order nonlinearities as they can found use in numerous opto-electronic applications.[1–4] Crystals can be very promising photonic materials with respect to applications.[5–7] Borate crystals are known as very effective nonlinear optical (NLO) materials for frequency conversion of laser emission from near-infrared (NIR) to the visible (VIS) or ultraviolet (UV), and vacuum-UV (VUV) spectral regions.[8] Some borate crystals doped with rare earth luminescence ions can generate selected wavelengths in NIR and/or VIS spectral range by the emission of excited luminescence ions.[9,10] Such bi-functional materials, in which the laser effect and the non-linear optical phenomena occur simultaneously inside the same host are very attractive for laser devices.[11]

$Bi_2ZnOB_2O_6$ crystallizes in the non-centrosymmetric orthorhombic space group Pba2. The crystal structure is formed by a three-dimensional network consisting of $ZnB_2O_7^{6-}$ layers alternating with six-coordinated Bi^{3+}cations along *c* axis. The unit-cell parameters of $Bi_2ZnOB_2O_6$ are: $a = 10.8200(7)$ Å, $b = 11.0014(7)$ Å, $c = 4.8896(3)$Å, $Z = 4$, $V = 582.03(6)$ Å^3.[12] Due to its structure, the $Bi_2ZnOB_2O_6$ has very attractive linear and nonlinear optical properties. It is an optically positive biaxial optical crystal with relatively large birefringence (0.085–0.106).[13] The second harmonic generation (SHG) coefficients d_{31}, d_{32}, d_{33} of $Bi_2ZnOB_2O_6$ single crystals grown by the Kyropoulos method[14] have been already determined using 1064 nm excitation.

In this work $Bi_2ZnOB_2O_6$ single crystals, due to their congruent melting near 690 °C and lack of unwanted phase transitions, were grown from stoichiometric melts by means of the Top Seeded Kyropoulos method similar to that described in Ref. 12. Growth was carried out in a two-zone resistance furnace under conditions of low temperature gradients. Temperature of the heating zones was controlled with Eurotherm 906S programmers. The lower zone controlled the temperature of the melt while the upper zone was mainly used to keep proper temperature gradient. The melt was slowly cooled at a rate equal to 0.02 K/h. No pulling was used, a $Bi_2ZnOB_2O_6$ crystal grew on a rotating seed in the volume of the melt and was confined with crystallographic faces. After the growth, the $Bi_2ZnOB_2O_6$ crystal was withdrawn from the melt and cooled to room temperature at a rate equal to 5 K/h. The seed was cut along the 100 direction. The morphology of the as-grown colorless $Bi_2ZnOB_2O_6$ crystal was investigated. Its main crystallographic faces were found to be {110} and {100}, forming crystal zone 001, and {100} and {001} ones, forming crystal zone 010. The dimensions of the $Bi_2ZnOB_2O_6$ slabs used for determining the NLO coefficients were $5.0 \times 5.0 \times 2.0$ mm^3.

It is important also to underline that from the point of view of material science properties and large scale production the $Bi_2ZnOB_2O_6$ melts congruently, and contrary to Barium borate (BBO) does not show irreversible high temperature phase transition, so can be grown from stoichiometric melts with good optical quality and relatively high yield. Moreover, the quality of BBO suffers from the use of additional solvents that are employed in order to lower the temperature of crystallization below the temperature of irreversible phase transition of beta to alfa phase at 925° C. Additionally, the flux growth of BBO is very slow. Comparing to Potassium Dihydrogen Phosphate (KDP) $Bi_2ZnOB_2O_6$ crystal is non-hygroscopic, which is an important factor. On the contrary due to the presence of the Bi ions, the absorption edge is shifted towards longer wavelengths.

The second and third order nonlinear optical response of the $Bi_2ZnOB_2O_6$ crystal has been measured by means of a second and third harmonic generation (SHG/THG) Maker fringes setup,[1,15–17] employing a Nd:YVO_4 laser with a repetition rate of 10 Hz delivering 30 ps laser pulses at 1064 nm.

a)E-mail: bouchta.sahraoui@univ-angers.fr

During the measurements, the second/third harmonic efficiency were measured as a function of the angle of incidence by gradually rotating the sample with a motorized rotational stage. The fundamental beam was cut off by means of a KG3 filer, while appropriate interference filters were used to selectively allow either the SHG or the THG signals to be detected. The obtained signals in both cases were detected by appropriate photomultiplier and averaged by a boxcar average. The acquisition was automatically done by a computer in Labview environment.

In the case of the SHG measurements, the reference material was a 0.5 mm thick Y-cut quartz slab ($d_{11} = 0.5$ pm/V and $L_c = 20.5\ \mu$m). The power of the second harmonic generated signal is given by the following equation and it is a function of the incident angle:[18]

$$P_{2\omega} = af(\theta)\sin^2(\psi), \tag{1}$$

where

$$\psi = \frac{\pi L}{2}\frac{4}{\lambda}(n_\omega \cos\theta_\omega - n_{2\omega}\cos\theta_{2\omega}). \tag{2}$$

In the previous equations, $\alpha f(\theta)$ is a function of the incident angle, L is the thickness of the sample, λ is the fundamental wavelength, n_ω, $n_{2\omega}$ are the refractive indices at ω and 2ω, respectively, and θ_ω and $\theta_{2\omega}$ are the corresponding refractive angles. Also, α is a constant given by the following equation:

$$\alpha = \frac{512\pi^2}{cw^2}d^2P_\omega^2, \tag{3}$$

where c is the speed of light in vacuum and w is the radius of the light beam. The coefficient d_{eff} can be determined from the following equation utilizing the maximum values of the Maker fringes:

$$\frac{d_{eff,sample}^2}{d_{eff,calibration}^2} = \frac{a_{sample}}{a_{calibration}}, \tag{4}$$

where a thin quartz slab has been utilized for the calibration purposes as previously described. In Figure 1(a), Maker fringe pattern can be seen for the $Bi_2ZnOB_2O_6$ crystal. By using the aforementioned model, the d_{eff} value was determined to be 0.25 pm/V, which is comparable to the response of the well-known KDP crystal.[19,20] In the work by Li and Pan,[14] the values of the SHG coefficients d_{31}, d_{32}, d_{33} of $Bi_2ZnOB_2O_6$ prepared by the Kyropoulos method have been determined under 1064 nm excitation to be 2.34, 7.90, and 2.60 times higher than the d_{36} coefficient of KDP crystal, respectively.

Moreover, a characteristic THG Maker fringes curve can be seen in Fig. 2. For the determination of the third order nonlinear susceptibility the following model was used, employing a 1 mm silica slab for calibration purposes.

The third order nonlinear susceptibility of the silica slab is $\chi^{(3)} = 2.0 \times 10^{-22}$ m^{2}V^{-2}. Briefly, the third harmonic generation intensity is given by the following equation:[17]

$$I^{3\omega} = Bf(\lambda_{3\omega})\left|\frac{\chi^{(3)}}{\Delta\varepsilon}\right|_S^2 (I^\omega)^3 \left| A\left(t_{12}^\omega\right)^3 \exp\left(i\psi_s^{3\omega}\right) \times \left\{\exp\left[i\left(\psi_s^\omega - \psi_s^{3\omega}\right)\right] - 1\right\} + C'\left\{t_{23}^{3\omega}\exp[i(\psi+\alpha)] - \left(t_{12}^\omega t_{23}^\omega\right)^3 \exp[-i(\psi+\beta)]\right\}\right|^2, \tag{5}$$

where $Bf(\lambda_{3\omega})$ depends on the experimental setup, $\Delta\varepsilon$ is the dispersion of the dielectric constant, I_ω is the intensity of the fundamental beam, A is a transmission factor through the sample, t are the transmission coefficients, $\psi_s^{3\omega}$, ψ_s^ω are the phase angles, α, β are phase factors, and C' is given by the following equation:

$$C' = \left[\frac{\chi^{(3)}}{\Delta\varepsilon}\right]_A \Big/ \left[\frac{\chi^{(3)}}{\Delta\varepsilon}\right]_S C. \tag{6}$$

The third order nonlinear susceptibility of the crystal, by using silica as calibration material was found to be 3.22×10^{-21} m^2 V^{-2}.

Moreover, two-dimensional images were obtained by means of a SHG microscopy setup, employing a Ti:Sapphire laser (Tsunami, Spectra Physics), which is tunable in the spectral region 700–1080 nm and providing 120 fs with 80 MHz repetition rate laser pulses. The measurements were

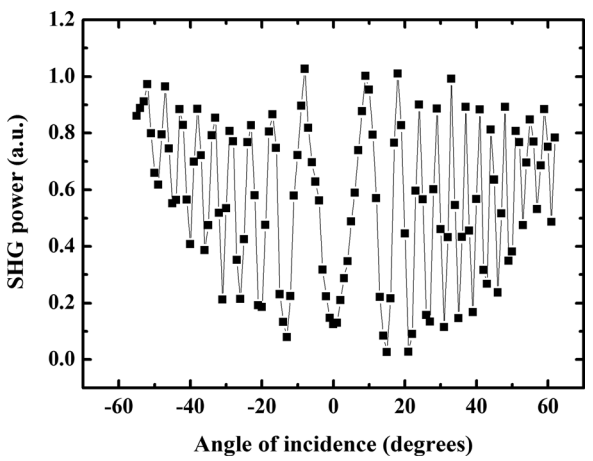

FIG. 1. SHG Maker fringes curve.

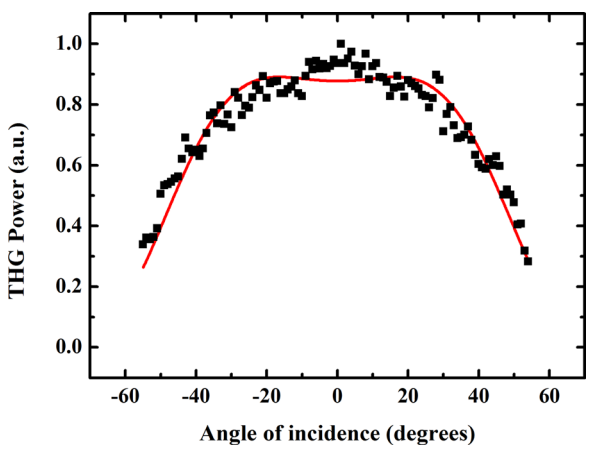

FIG. 2. THG Maker fringes curve.

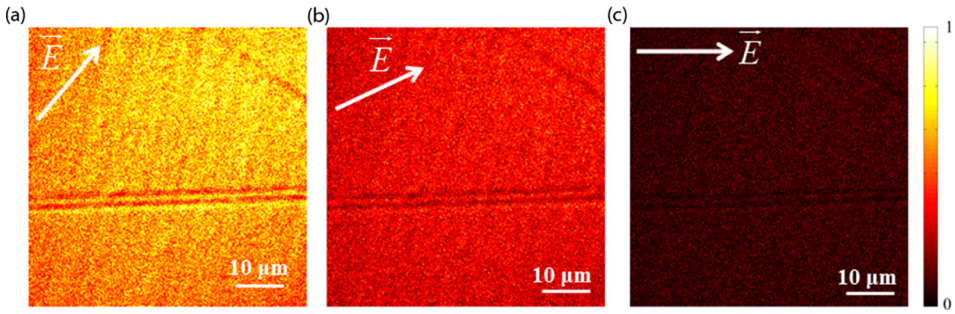

FIG. 3. SHG images as a function of polarization. 3(a) Polarization at 50° with respect to p polarization, corresponding to SHG maximum. 3(b) polarization at 25° with respect to p polarization, corresponding to intermediate SHG signal. 3(c) p polarization corresponding to SHG minimum.

carried out at 800 nm, while the laser beam has been focused on the sample by a 50× objective of an inverted, modified microscope (IX 71, Olympus). The size of the laser beam on the focal plane was about 1 μm. The angular deviation of the beam has been controlled by means of an X-Y scanner, which is composed of two galvanometric mirrors. The SHG signal has been filtered out and detected by a photon counter. The power and the polarization of the beam, the amplitude of the galvanometric mirrors, and the positioning of the samples have been precisely adjusted by means of a homemade Labview program. With the same program, the SHG signal for every position of the laser beam on the sample has been stored in order to provide finally the 2D-SHG images.

In this way, several 2-D SHG images (200 × 200 pixels) of the crystal were obtained as a function of the incident laser polarization. The exposure time for each pixel was 20 μs, the laser excitation wavelength was 800 nm (laser power: 40 mW). In particular, one image has been stored for every 2 degrees of rotation. In Fig. 3, three characteristic images can be seen corresponding to p polarization (image 3(c)), 50° (image 3(a)), and 25° (image 3(b)) with respect to p polarization.

By averaging the signal of each image, the SHG intensity for each polarization angle has been found and the normalized SHG intensities are presented in Fig. 4 as a function of the polarization angle. In the same figure, the positions corresponding to the images of Fig. 3 can be seen. A SHG maximum has been found at an angle of 50° with respect to p polarization while minimum SHG has been obtained for p polarization.

In this work, we have grown high quality $Bi_2ZnOB_2O_6$ crystals. The SHG and THG response of the $Bi_2ZnOB_2O_6$ crystal was studied by the Maker fringes techniques. By using SHG microscopy, two dimensional images of the second order nonlinearity were obtained as a function of the incident polarization providing the dependence of the SHG intensity on the incident polarization. The crystals have been shown to have high SHG and THG efficiency, comparable with those of well-known crystals such as BBO, KDP. Our preliminary investigations, which are currently in progress show that $Bi_2ZnOB_2O_6$ may be efficiently doped with rare earth elements (RE) ions. In this way, the produced systems will be able to emit selected wavelengths in the near infrared and in the visible spectral range by the emission of excited luminescent ions (down- and up-conversion progress) and by SHG. The aforementioned features of the investigated $Bi_2ZnOB_2O_6$ make them very attractive materials for applications.

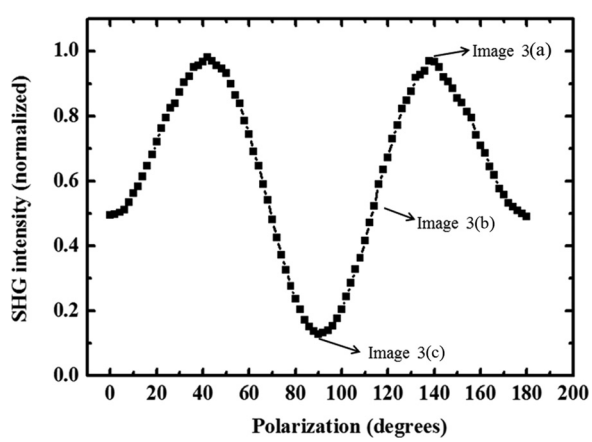

FIG. 4. Normalized SHG intensity as a function of the incident polarization.

K.I. acknowledges support from the European Commission and General Secretariat for Research and Technology (Greece) for a National Strategic Reference Framework (NSRF) Project (PE3-(1612)). D.K. acknowledges support by the Research Project of the Polish Ministry of Sciences and Higher Education: DS-PB/64-001/13. A.M. acknowledges support of the Polish Ministry of Sciences and Higher Education, Key Project POIG.01.03.01-14-016/08-08 "New Photonic Materials and Their Advanced Application" in 2013.

[1]H. El Ouazzani, K. Iliopoulos, M. Pranaitis, O. Krupka, V. Smokal, A. Kolendo, and B. Sahraoui, J. Phys. Chem. B **115**, 1944 (2011).
[2]Z. Essaidi, O. Krupka, K. Iliopoulos, E. Champigny, B. Sahraoui, M. Sallé, and D. Gindre, Opt. Mater. **35**, 576 (2013).
[3]K. Iliopoulos, A. El-Ghayoury, B. Derkowska, A. Ranganathan, P. Batail, D. Gindre, and B. Sahraoui, Appl. Phys. Lett. **101**, 261105 (2012).
[4]K. Iliopoulos, R. Czaplicki, H. El Ouazzani, J. Y. Balandier, M. Chas, S. Goeb, M. Sallé, D. Gindre, and B. Sahraoui, Appl. Phys. Lett. **97**, 101104 (2010).
[5]M. Derbazi, A. Migalska-Zalas, G. Goldowski, I. V. Kityk, H. El Ouazzani, J. Ebothe, and B. Sahraoui, Opt. Mater. **34**, 1261 (2012).
[6]B. Sahraoui, R. Czaplicki, A. Klopperpieper, A. S. Andrushchak, and A. V. Kityk, J. Appl. Phys. **107**, 113526 (2010).
[7]B. Kulyk, V. Kapustianyk, Ya. Burak, V. Adamiv, and B. Sahraoui, Mater. Chem. Phys. **120**, 114 (2010).
[8]C. Chen, T. Sasaki, R. Li, Y. Wu, Z. Lin, Y. Mori, Z. Hu, J. Wang, G. Aka, M. Yoshimura, and Y. Kaneda, *Nonlinear Optical Borate Crystals: Principals and Applications*, (Wiley-VCH Verlag&Co., Wenheim, Germany, 2012).
[9]M. N. Palatnikov, I. V. Biryukova, N. V. Sidorov, A. V. Denisov, V. T. Kalinnikov, P. G. R. Smith, and V. Ya. Shurd, J. Cryst. Growth **291**, 390 (2006).
[10]S. Zhao, J. Yao, E. Zhang, G. Zhang, J. Zhang, P. Fu, and Y. Wu, Solid State Sci. **14**, 305 (2012).
[11]A. Brenier, D. Jacque, and A. Majchrowski, Opt. Mater. **28**, 310 (2006).

[12]F. Li, X. Hou, S. Pan, and X. Wang, Chem. Mater. **21**, 2846 (2009).
[13]F. Li, S. Pan, X. Hou, and J. Yao, Cryst. Growth Des. **9**, 4091 (2009).
[14]F. Li and S. Pan, J. Cryst. Growth **318**, 629 (2011).
[15]W. N. Herman and L. M. Hayden, J. Opt. Soc. Am. B **12**, 416 (1995).
[16]J. Jerphagnon and S. K. Kurtz, J. Appl. Phys. **41**, 1667 (1970).
[17]X. H. Wang, D. P. West, N. B. McKeown, and T. A. King, J. Opt. Soc. Am. B **15**, 1895 (1998).
[18]X. Zhang, X. Wang, G. Wang, Y. Wu, Y. Zhu, and C. Chen, J. Soc. Opt. Am. **24**, 2877 (2007).
[19]W. J. Alford and A. V. Smith, J. Opt. Soc. Am. B **18**, 524 (2001).
[20]R. J. Gehr and A. V. Smith, J. Opt. Soc. Am. B **15**, 2298 (1998).